A Fluorescent Probe for STED Super-Resolution Imaging of Vicinal-Dithiol-Proteins (VDPs) on Mitochondrial Membrane

Zhigang Yang, Dong Hoon Kang, Hoyeon Lee, Jinwoo Shin, wei yan, Bhowmira Rathore, Hye-Ri Kim, Seo Jin Kim, Hardev Singh, Liwei Liu, Junle Qu, Chulhun Kang, and Jong Seung Kim

Bioconjugate Chem., **Just Accepted Manuscript** • DOI: 10.1021/acs.bioconjchem.8b00128 • Publication Date (Web): 23 Mar 2018

A Fluorescent Probe for STED Super-Resolution Imaging of Vicinal-Dithiol-Proteins (VDPs) on Mitochondrial Membrane

Zhigang Yang,[†,‡,§] Dong Hoon Kang,[¶,§] Hoyeon Lee,[#,§] Jinwoo Shin,[‡,§] Wei Yan,[†] Bhowmira Rathore,[†] Hye-Ri Kim,[#] Seo Jin Kim,[#] Hardev Singh,[‡] Liwei Liu,[†] Junle Qu,[†,*] Chulhun Kang,[#,*] and Jong Seung Kim[†,‡,*]

[†]Key Laboratory of Optoelectronic Devices and Systems of Ministry of Education and Guangdong Province, College of Optoelectronic Engineering, Shenzhen University, Shenzhen, Guangdong 518060, China.

[‡]Department of Chemistry, Korea University, Seoul 02841, Korea.

[¶]Asan Medical Center, College of Medicine, University of Ulsan, Seoul 138-736, Korea.

[#]The School of East-West Medical Science, Kyung Hee University, Yongin, Gyeonggi-do 17104, Korea.

§These authors contributed equally to this work.

E-mail: jlqu@szu.edu.cn (J. Qu); kangch@khu.ac.kr (C. Kang); jongskim@korea.ac.kr (J. S. Kim)

Abstract

Realizing the significant roles of vicinal-dithiol proteins (VDPs) in maintaining the cellular redox homeostasis and their implication in many diseases, we synthesized a smart arsenate based fluorescent probe **1** which can preferentially target the mitochondrial membrane-bound vicinal dithiol proteins (VDPs), especially voltage-dependent anion channel (VDAC2). The probe targetability was demonstrated by ''*in vitro*'' studies such as co-localization, stimulated emission depletion (STED) super-resolution imaging, proteomic MS/MS analysis and by western blot analysis. The probe represents a rare example of fluorescence labeling of mitochondrial membrane-bound VDPs and can provide a new way to construct VDPs-specific fluorescent probes to gain deeper understanding of their roles in mitochondrial-related disorders.

Introduction

Vicinal dithiol proteins (VDPs) are proteins where two cysteine residues are proximal in their primary structures, for example, CXXC, and the residues may act as molecular switch depending on the cellular redox potential through formation of the corresponding disulfide bonds. The VDPs have received significant attention because of its fundamental roles in various biological processes including protein folding and stabilization of its native structure, maintaining cellular redox homeostasis and regulation of mitochondrial functions.[1-5] Moreover, VDPs are also recognized to be implicated in many human diseases such as cancer, diabetes, platelet function, human immunodeficiency virus type 1 (HIV-1), neurodegeneration and so forth.[6-10]

Mitochondria have abundant VDPs, which are estimated as 5–15% of the total protein thiols[11] and are presumed to play a significant role in mitochondrial antioxidant defences and in redox signalling.[12,13] Taking advantages of arsenicals such as 1, 3, 2-dithiarsenolane to selectively bind to the vicinal dithiols

in proteins,[14-15] a arsenical-based fluorescent probe was developed to label VDPs *in situ* in live cells.[16-18] Interestingly, the probe seems to prefer the mitochondrial VDPs even without any mitochondrial targeting unit such as a triphenylphosphonium group which may be attributed to relatively high VDP contents.

Among the mitochondrial VDPs, the membrane VDPs deserve much attention based on the following two considerations: i) the significant portion of mitochondrial VDPs is found on membrane,[19] and ii) the on-off switching of permeability transition pore complex in mitochondrial membrane is susceptible to alter redox environments and further to trigger cell apoptosis.[20, 21] Likely, mitochondrial membrane-bound VDPs may be involved in pathogenic events in the organelle. In this regard, development of a fluorescent probe targeting mitochondrial membrane-bound VDP's would provide valuable information for understanding the role of mitochondrial redox balance in various mitochondria-related human diseases, which has not been attempted so far.

Accordingly, we successfully synthesized a fluorescent probe **1** in which a BODIPY based fluorophore, on one end, is conjugated to triphenylphosphonium group (a typical mitochondrial targeting unit) *via* an alkyl spacer which provides suitable lipophilic character for membrane localization, and on other end it was conjugated to phenylarsenicate (a recognition site for VDPs) particularly for imaging and labelling the VDP's on mitochondrial membranes.

Results and discussion

The BODIPY probe **1** was prepared according to the protocols reported in our previous work[22] with some modifications. The complete synthetic scheme and the synthetic details are described in Scheme 1. Briefly, 4-hydroxyphenyl-tetramethyl BODIPY (**6**) was obtained from 4-hydroxybenzaldehyde (**7**) in 20% yield. Then, alkylation of **6** with 1,6-dibormohexane to produce **5**, followed by Vilsmeier-Hacck reaction resulted in the formation of aldehyde derivative **4**. Compound **3** was obtained by refluxing

mixture of **4** and triphenylphosphine in toluene for 12 hours and finally condensed with arsenical **8** and non-arsenical derivative through a base-catalysed reaction to yield target compound **1** and reference compound **2** in moderate yields, respectively.

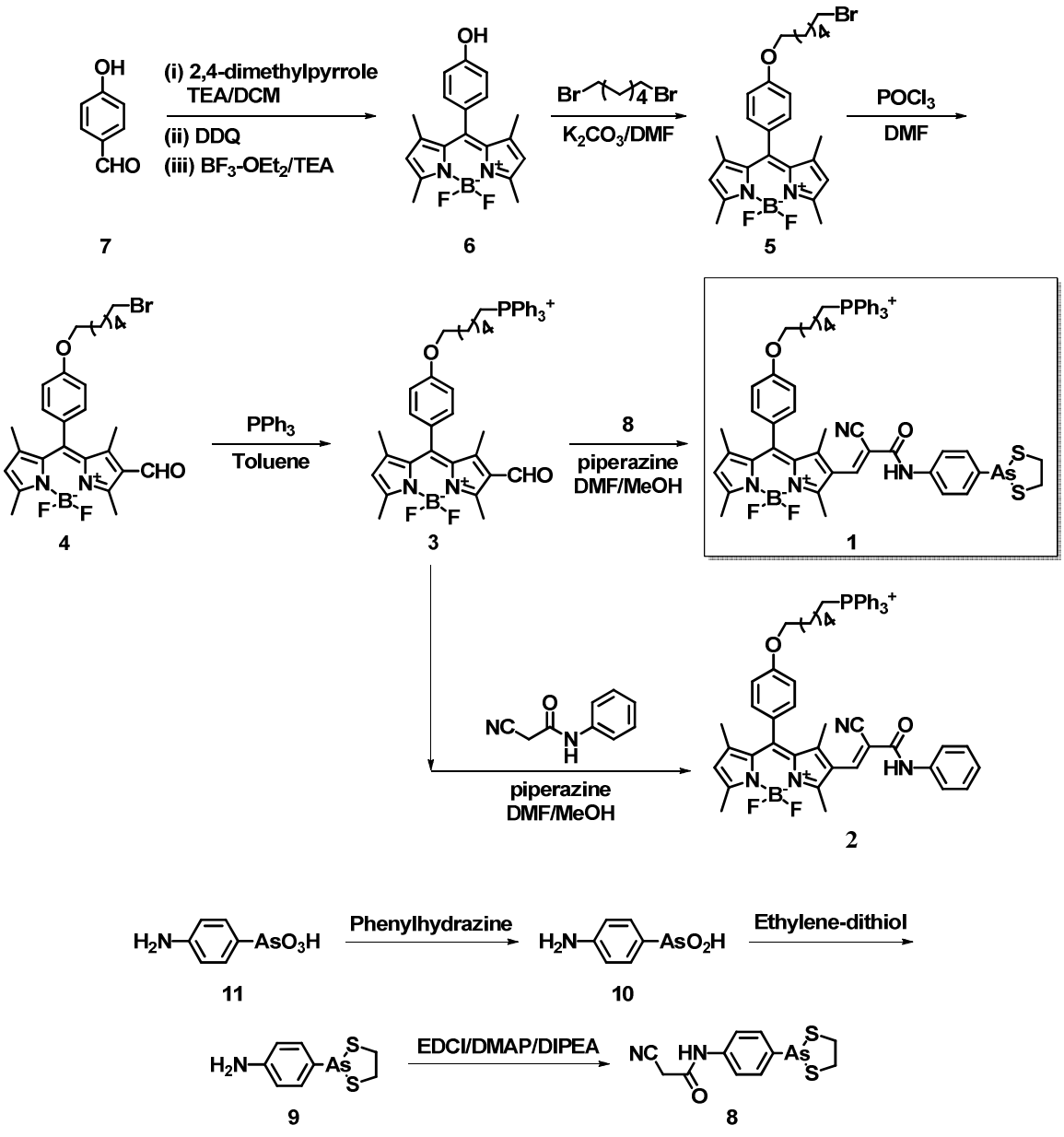

Scheme 1. Synthetic route of target compound **1** and reference compound **2**.

As shown in Figure 1, probe **1** in methanol exhibits absorption and emission maxima at 513 and 534 nm, respectively. The spectra for reference compound **2** are almost identical to those of **1**, indicating that the organoarsenic moiety does not affect the BODIPY's spectral behaviours (Figure S1). In addition, the emission of **1** was insensitive to solvent polarity as it displayed negligible shift in its emission maxima in different solvents (Figure S2). Moreover, as suggested by confocal fluorescence images, cells incubated with probe **1** displayed intense green fluorescence intensity and it was anticipated that fluorescence signals intensified as the time of incubation increases. These results collectively indicate that probe **1** showed efficient labelling properties towards VDP's and fluorescence intensity is directly proportional to degree of VDP's modification by organoarsenic moiety of probe **1**.

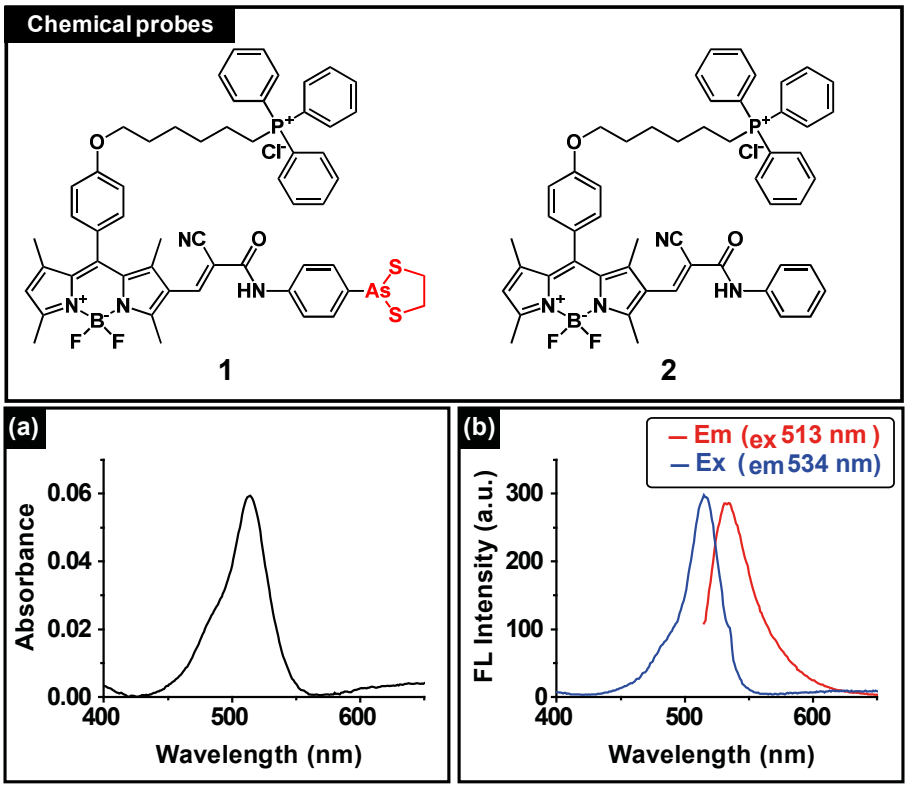

Figure 1. Chemical structures of target probe **1** and reference compound **2.** The absorption (a), fluorescence (red in b) and excitation (blue in b) spectra of **1** (1.0 μM) in methanol; The emission

spectrum was taken upon excitation at 534 nm and the excitation spectrum was obtained with emission at 514 nm.

In order to demonstrate whether **1** can selectively react with vicinal dithiol motifs of proteins, the reduced and oxidized form of bovine serum albumin (rBSA and oBSA) were prepared by treating it with 1,4-dithiothreitol (DTT) and hydrogen peroxide (H_2O_2), respectively.[23] Then, BSAs were allowed to react with probe **1** and their products were analyzed using SDS-PAGE. The gel electrophoretic profiles of the reaction mixtures of BSAs with probe **1** are shown in Fig. 2a, where the protein bands were visualized using CBB G250 staining or by following the probe **1** emission. As shown in Fig. 2a, although the similar intensities on the CBB-stained image were observed for both BSAs, single fluorescent band was found only on the rBSA-loaded lane. Considering that a strong detergent (SDS) was applied to the experimental condition for the gel electrophoresis, the emission on the gel is not due to any non-covalent complex between the probe and proteins, but due to covalent bonding of probe **1** with rBSA, presumably through its reaction with rBSA's vicinal dithiol groups.

To verify that probe **1** can covalently modify the cellular VDPs in live cells, HeLa cells were incubated with **1** or **2** for 1 hour and the images were recorded using confocal laser fluorescence microscopy (Figures 2b, S3, S4). The confocal images of both **1** and **2**-treated HeLa cells showed strong green signals after 1 h-incubation as shown in left panel of Figure 2b. However, after a sequential washing steps with PBS/50% ethanol (1:1 *v*/*v*)/formaldehyde solution, only the **1**-treated cells displayed persistent fluorescence intensity (Figures 2b and S3), while the intensity from **2**-treated cells was dramatically reduced, attributing to the non-covalent interaction between **2** and the cell matrix. This suggests that the fluorescence of **1**-treated cells is mostly aided by covalent labelling of the cellular macromolecules, presumably the vicinal dithiol proteins. Quantization of the fluorescence intensities (Figures 2c, S3) further validates this conclusion. Further, we also investigated the effect of phenylarsinoxide (PAO), a well-known modifier of VDPs[24] on the **1**-lavelling of the cells. The intensity

of the confocal images of **1**-treated cells in the presence of PAO displayed gradually decrease in a dose-dependent manner (Figure S4), implying that the modification by **1** is directed to VDPs.

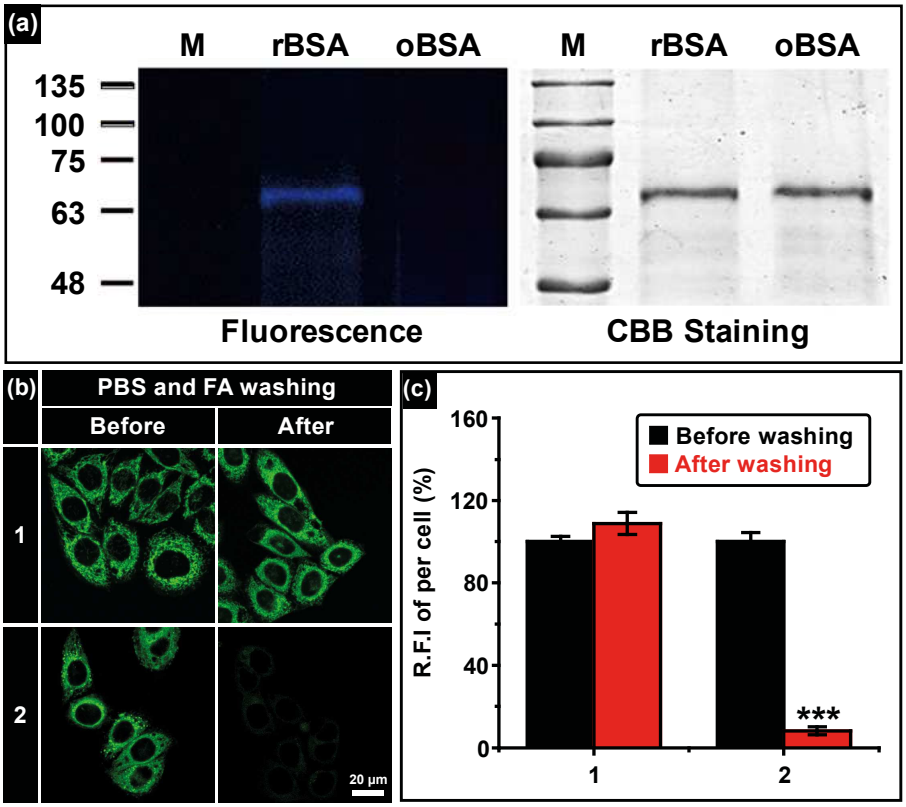

Figure 2. SDS-PAGE of rBSA and oBSA after reaction with **1** and fluorescent labelling of **1** and **2** (1.0 μM) for 1 hour (37 °C, 5% CO_2); Fluorescent and CBB G250 stained images were taken from a SDS-PAGE gel; (a) Protein size markers are shown on M lane. The amount of BSAs on the panel (a) was 1 μg per lane and the fluorescent images were obtained using a fluorescence scanner (Typhoon FLA 9400, GE), excited at 488 nm, collected at 500-540 nm; (b) Fluorescent images of HeLa cells were obtained before and after 1×PBS washing followed by ethanol (1:1 ratio) and three rounds of 4% formaldehyde solution; (c) Histogram of relative fluorescence intensity (R. F. I.) per cell was represented using image J program. Results represent the mean (± SEM) of three independent experiments (n = 3). The statistical signification was marked as *** for $p < 0.001$, compared with each of the fluorescence intensity before

washing.

Identification of the intracellular location of **1** would be a reasonable step for further investigation of mitochondrial VDPs which was performed with fluorescence co-localization experiments using various organelle markers (*i.e.*, Mito-, Lyso-, and ER-trackers). As seen in Figure 3, the fluorescent image of **1**-treated cell is well overlapped with that of Mito-tracker as compared to Lyso- and ER-trackers with Pearson's correlation coefficient values are 0.89, 0.41, and 0.51 for the Mito-, Lyso-, and ER-trackers respectively. The preferential mitochondrial localization is attributed to its triphenylphosphonium group, a well-known mitochondrion guiding unit due to the positively-charged bulky hydrophobic moiety.[25-27] Taken together, these results demonstrated that **1** is localized into the mitochondria and covalently modify the macro-molecules, most likely the reduced forms of its vicinal dithiol proteins.

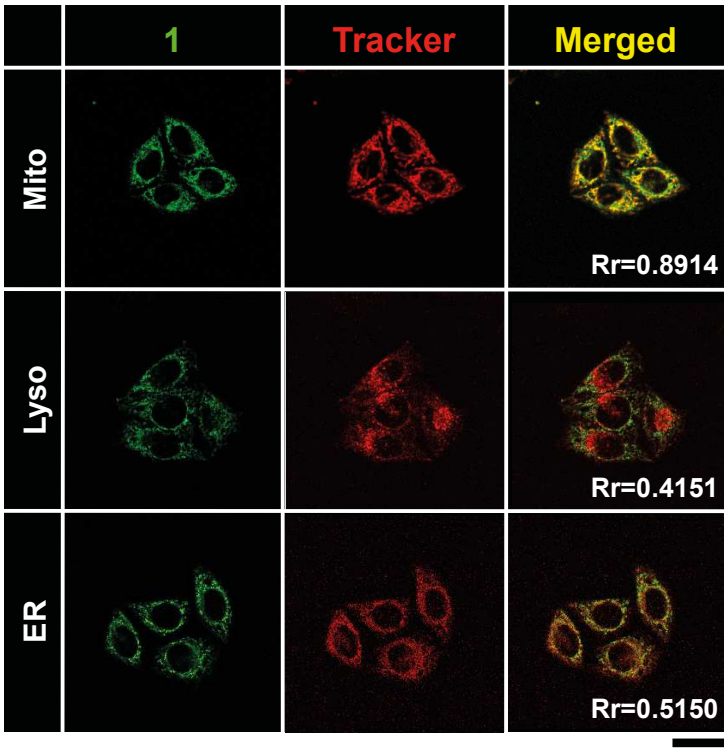

Figure 3. Co-localization images of **1** (1.0 μM) in HeLa cells co-treated with organelle staining dye [Mito-Tracker Red (0.1 μM) or Lyso-Tracker Red (0.1 mM) or ER-Tracker Red) (0.2 μM)]. Scale bar indicates 50 μm. Rr = Pearson's correlation coefficient.

Further, to evaluate whether the fluorescent labelling by **1** is sensitive to oxidative stress of mitochondria, confocal fluorescence images were recorded in the presence of oligomeric $A\beta_{1-42}$, a well-known mitochondrion damaging agent.[28-31] As shown in Figure 4, the $A\beta_{1-42}$ treatment induced the dramatically increased ROS production in mitochondria, which were visualized by increased red signals of MitoSOX, a mitochondrial superoxide indicator. This result indicates that the $A\beta_{1-42}$ treatment indeed provokes ROS generation in mitochondria to the cells. The subsequent addition of **1** to the oligomeric $A\beta_{1-42}$-treated cells showed significantly reduced fluorescence intensity as compared to that without $A\beta_{1-42}$ treatment. However, it is interesting that under similar conditions the change in fluorescent intensity of Mito-Tracker was negligible (Figure S5), indicating that the cells maintain the mitochondria membrane potentials yet. Nonetheless, the dramatic reduction of **1**'s emission may be attributed to the increased oxidized forms of mitochondrial VDPs upon $A\beta_{1-42}$ treatment; thereby implicates that probe **1** is highly sensitive to the reduced state of mitochondrial VDPs.

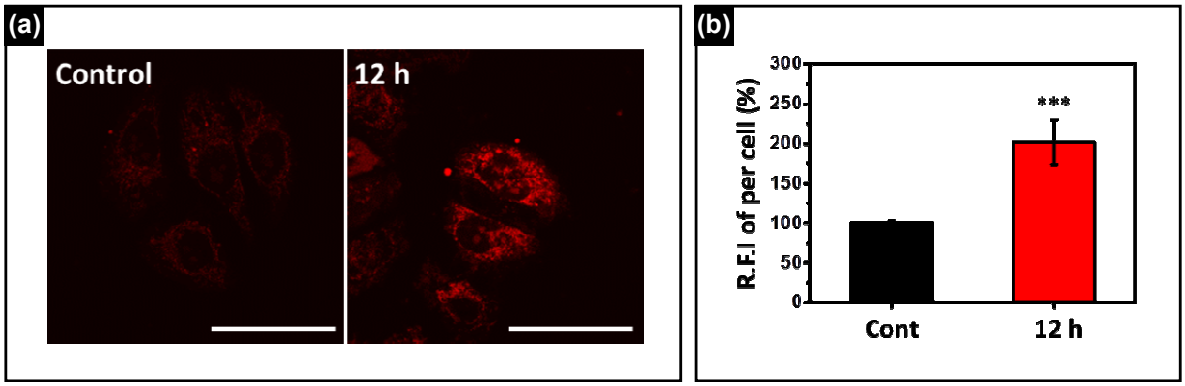

Figure 4. Confocal microscopic images of HeLa cells co-labelled with oligomeric $A\beta_{1-42}$ (a mitochondrial damaging agent) and MitoSOX (red emissive mitochondrial ROS indicator) as function of incubation time. Cells were seeded at 35 mm confocal dish. Cells were pretreated with oligomeric $A\beta_{1-42}$ (10.0 μM) for 12 h in incubator (37 °C, 5% CO_2). After each time of incubation, cells were co-labeled with MitoSOX (2.0 μM) in 1×PBS for 20 min at 37 °C in dark. The fluorescent confocal images were collected using an excitation wavelength of 488 nm and a long-path 530 nm emission filter and compared with oligomeric $A\beta_{1-42}$ untreated control cells. Scale bar indicate 50 μm. Histogram of relative fluorescence intensity (R. F. I.) per cell was represented using image J program. Results represent the mean (± SEM) of five independent experiments (n = 5). The statistical signification was marked as *** for $p < 0.001$.

In order to further confirm the exact localization of **1** in mitochondria, we used time gated STED (stimulated emission depletion) super resolution imaging microscope to observe the fine structure of mitochondria using fluorescent imaging. First, it is significant to test STED depletion ability of **1** in live cells. HeLa cells were incubated with **1** (2 μM) for 30 minutes and then upon excitation at 514 nm (1% of excitation Laser power), different STED laser powers at 592 nm were used to test the stimulated depletion effect. It was demonstrated that 10% of STED laser power is enough to acquire marked depletion in fluorescence imaging (Figure S6).

The STED super resolution imaging showed much clear cellular imaging with enhanced imaging resolution of *ca.* 170 and 84 nm at 10% and 40% of STED Laser power, respectively (Figures S7 and S8). As shown in Figure 5, compared to the confocal imaging (FWHM > 250 nm in Figure 5A, 5E Black line), STED CW laser at 10% of laser power provided high resolution image (Figure 5B). After a series of image optimization steps as shown in Figure 5C, a fine fluorescence images of mitochondria with *ca.* 90 nm resolution was obtained (Figure 5D). The image shows tubular appearance with spotted

labelling which is anticipated for modification of clustered proteins on membrane rather than mitochondria matrix proteins which would appear as continuous features. Likewise, this result suggests that **1** can specifically labelled the VDPs localizing on the mitochondrial membrane in HeLa cells.[32]

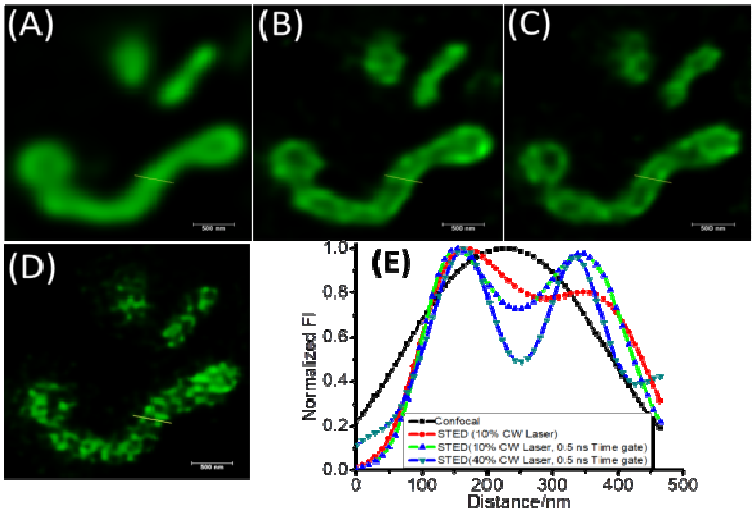

Figure 5. (A) Confocal fluorescence of selected mitochondria; (B) STED super resolution image of mitochondria recorded with 10% energy power of STED laser; (C-D) STED super resolution images recorded with 10% (C) and 40% (D) of STED laser power at 592 nm after switching on the time gate to eliminate the background fluorescence with lifetime less than 0.5 ns; (E) Line traces through the single mitochondrial segment show the markedly improved resolving power of STED; excitation wavelength was 514 nm with 1% of Laser power and depleted Laser wavelength was 592 nm with 10% (B, C) and 40% (D) of energy power of CW Laser source. These optical properties were measured on a Leica SP8 fluorescent imaging system.

To identify the **1**-modified proteins in the cells, a proteomic mass spectral (MS) analysis was carried out for the fluorescently labelled band of SDS-PAGE of mitochondrial fractionation. After incubation with **1**, HeLa cells were fractionated into three subcellular compartments (cytosol, mitochondria and nuclei) according to the protocol provided by the supplier. The purities of the obtained fractions were verified by SDS-PAGE-based Western blot analysis using organelle-selective proteins markers (Figure

S9). The gel for three fractions was subjected to fluorescence imaging and CBB-staining (Figure 6a). As anticipated from the confocal microscopic study, the fluorescent intensity of the lanes showed strong for the mitochondria fraction. Moreover, surprisingly, there is a major band on the fluorescence image of the gel and its intensity was diminished upon oligomeric $A\beta_{1\text{-}42}$ treatment. This result implies that the fluorescent image of the cells by **1** is mostly contributed by modification of single VDP in mitochondrial membrane and the VDP's redox state seems to be involved in mitotoxicity by $A\beta_{1\text{-}42}$. Therefore, the peptides collected from the fluorescent band on SDS-PAGE gel were applied to MS/MS analysis. The analysis suggests 12 protein names as Voltage-dependent anion channel (VDAC2) (Figure S9). Considering the proteins; molecular weight, location, and roles in mitochondria, the best candidate for the bands in Figure 6 would be VDAC2 where Figure S9 shows any significant change in its total expression level (Figures 6b, S9). These results suggest that the vicinal thiols in VDAC2 behaves as a molecular sensor for redox environment in mitochondria.[33-37]

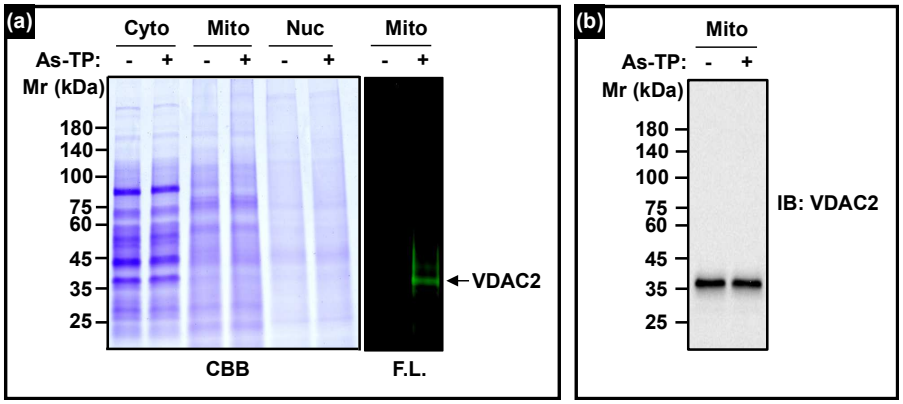

Figure 6. Identification of **1**-modified proteins in mitochondrial fraction of HeLa cells; (a) HeLa cells were incubated with 2 μM of As-TP for 1 hour; three subcellular fractions from HeLa cells were separated on a 10% SDS-PAGE gel and the fluorescence image of gel was taken by Typhoon 9400 variable mode imager with 100 μm resolutions (Amersham Bioscience/GE Healthcare). After

fluorescence imaging, the gel was CBB-stained and merged with the corresponding fluorescence image for excision of protein band with the same position of electrophoretic mobility on SDS-PAGE gel; Cyto, cytosol; Mito, mitochondria; Nuc, nuclei; (b) Mitochondrial fractions from HeLa cells were immunoblotted using an anti-VDAC2 antibody. Shown is a representative of three independent experiments.

Conclusion

A phenylarsenicate-based fluorescent probe **1** was developed for highly selective and robust staining of VDPs on mitochondrial membrane. The probe can predominantly bind to vicinal dithiol proteins in mitochondria by covalent interactions between the arsenicate moiety and the reduced dithiols in proteins. STED super resolution imaging of live HeLa cells using the phenylarsenicate-based fluorescent probe **1** provided clear fluorescent profiles of mitochondrial membrane. Furthermore, probe **1** was proven to preferentially target the VDAC2 on the mitochondrial membrane *via* covalent binding of its arsenicate moiety to the vicinal dithiols, which was verified by different approaches, *e.g.* the comparison of SDS-PAGE of rBSA and oBSA, colocalization imaging, proteomic MS/MS analysis and Western blot analysis. Releasing the important roles played by mitochondrial VDPs as mentioned above, we believe that our system will have significant contribution to understand various diseases resulted from the malfunctions of VDAC2.

Experimental section

Synthesis of 4-aminophenylarsenoxide (10). Compound **10** was prepared according to the literature procedure. *p*-Arsanilic acid **(11)** (22 g, 100 mmol) was dissolved in methanol (100 mL) and heated to reflux. Phenylhydrazine (23 mL, 220 mmol) was titrated dropwise to above mixture in 30 minutes.

When N_2-production ceases, refluxing was continued for 1 h. The mixture was condensed at 80^{o}C to exclude the solvent, then washed with water (100 mL) and an aqueous NaOH solution (0.2 M, 60 mL) and finally with diethyl ether (2×150 mL). The aqueous solution was treated with aqueous NH_4Cl solution (5 M, 80 mL) suspended overnight at 0^{o}C. Precipitates were collected through a Büchner funnel filter, washed by ice-water (25 mL×2) and dried over KOH, which gave **10** as white powder (6.5 g, 26% yield).

Synthesis of 2-p-aminophenyl-1,3,2-dithiarsenolane (9) To a solution of **10** (2.6 g, 13 mmol) in dry ethanol (25 mL), ethanedithiol (1.5 mL, 20 mmol) was added dropwise and heated to reflux for 20 minutes with constant stirring. The solution was chilled in dry ice/acetone, co-distilled with toluene (106 mL) and concentrated. A white crystal was recrystallized from ethanol yielding 1.8 g (34% yield) of **9**. ^{1}H NMR (DMSO-d_6, 400 MHz): δ 3.13-3.36 (m, 4H), 5.40 (s, N-H, 2H), 6.56 (d, 2H, J = 8.8 Hz), 7.27 (d, 2H, J = 4.8 Hz) ppm.

Synthesis of compound 8. In 50 ml round bottom flask, 2-cyanoacetic acid (0.86 g, 10 mmol), EDCI (1 g, 7 mmol), DMAP (0.12 g, 1mmol) and DIPEA (0.5 mL) were added in DMF (20 mL) and the mixture was stirred for few minutes at room temperature. Then, amine **9** (1.3 g, 5 mmol) dissolved in DMF was added dropwise to above solution and stirring was continue overnight at room temperature. The reaction mixture was poured into saline solution (70 mL) and extracted with DCM (100 mL), dried over anhydrous Na_2SO_4. After evaporation of the DCM, the product was purified by column chromatography to provide product **8** (1.3 g, yield 80%). ^{1}H NMR (DMSO-d_6, 400 MHz): δ 3.11 (t, CH_2, 2H, J = 6.0 Hz), 3.28 (t, CH_2, 2H, J = 6.0 Hz), 3.84 (s, CH_2, 2H), 7.50-7.60 (dd, ArH, 4H, J = 8.0 Hz), 7.89 (s, NH, 1H); ^{13}C NMR (DMSO-d_6, 100 MHz): δ 31.40, 36.49, 42.09, 49.41, 116.38, 119.63, 132.15, 138.85, 161.81 ppm.

Synthesis of compound 6. 4-Hydroxybenzaldehyde (3.0 g, 24 mmol) and 2, 4-dimethylpyrrole (5 mL) were mixed in 10 mL freshly dried DCM followed by addition of 0.1 mL TFA at 0 ^{o}C under Ar-atmosphere. After stirring the resulting mixture overnight, DDQ (2.8 g) was added and stirred continuously for one hour more. Finally, $BF_3 \cdot OEt_2$ (3 mL) and TEA (6 mL) were added into the reaction mixture with stirring for additional 5 hours. Upon the completion of reaction, the raw product was separated by silica gel chromatography (hexane-DCM as eluent phase) to give the product of **6** (1.8 g, 21%).

Synthesis of compound 5. Compound **6** (1.4 g, 4 mmol), 1, 6-dibromobexane (2.0 g, 8 mmol) and K_2CO_3 (0.6 g, 4 mmol) were stirred in 15 mL dry DMF at 50 °C overnight. The product was separated through silica gel chromatography (DCM-methanol) to give **5** (1.6 g, 80%). ^{1}H NMR ($CDCl_3$, 400 MHz): δ 1.38 (s, CH_3, 6H), 1.48 (m, 4H, CH_2), 1.78 (m, 2H, CH_2), 1.82 (m, 2H, CH_2), 2.49 (s, 6H, CH_3), 3.38 (t, 2H, CH_2, J = 4.0 Hz), 3.95 (t, 2H, CH_2, J = 4.0 Hz), 5.92 (s, 6H, CH_3), 6.93 (d, 2H, ArH, J = 8.0 Hz), 7.05 (d, 2H, ArH, J = 8.0 Hz); ^{13}C NMR ($CDCl_3$, 100 MHz): δ 14.76, 14.81, 25.52, 28.17, 29.29, 32.87, 34.09, 68.02, 115.26, 121.33, 126.89, 129.30, 132.02, 142.22, 143.38, 155.28, 159.83 ppm.

Synthesis of compound 4. $POCl_3$ (1.54 g, 10 mmol) was dropped into dry DMF (6 mL) at 0 °C, over a period of 30 minutes. Then, **5** (1.6 g, 3 mmol) dissolved in 3 mL dry DMF was added into above solution, and the obtained mixture was heated at 60 °C for 5 hours. After cooling down to room temperature, the mixture was poured into ice-water (100 mL), and then neutralized with $NaHCO_3$. The crude product was extracted with DCM and purified through silica gel chromatography (DCM-methanol mixture solvent) to give **4** (1.2 g, 75.5%). ^{1}H NMR ($CDCl_3$, 400 MHz): δ 1.49 (s, CH_3, 3H), 1.55 (m, 4H, CH_2), 1.72 (s, 3H, CH_3), 1.92 (m, 4H, CH_2), 2.61 (s, 3H, CH_3), 2.82 (s, 3H, CH_3), 3.45 (t, 2H, CH_2, J = 4.0 Hz), 4.03 (t, 2H, CH_2, J = 4.0 Hz), 6.15 (s, 1H, CH_3), 7.03 (d, 2H, ArH, J = 8.0 Hz), 7.16 (d, 2H,

ArH, J = 8.0 Hz); 10.01 (s, 1H, CHO); ^{13}C NMR ($CDCl_3$, 100 MHz): δ 12.00, 15.34, 25.57, 26.88, 28.10, 29.25, 32.68, 33.99, 45.23, 68.14, 115.39, 124.07, 126.13, 129.39, 134.72, 143.06, 144.05, 147.54, 148.23, 156.56, 160.22, 161.61, 186.17 ppm.

Synthesis of compound 3. Compound **4** (1.1 g, 2 mmol) was placed in toluene (20 mL) together with triphenylphosphine (1 g, 3.8 mmol) and the obtained reaction solution was heated at 80 °C for 8 hours. After cooling down to ambient temperature, mixture was diluted with diethyl ether (150 mL) to precipitate the crude product which was filtered-off and washed with excess diethyl ether to get pure product **3** (1 g, 70%). ^{1}H NMR ($CDCl_3$, 400 MHz): δ 1.21 (bp, CH_2, 2H), 1.26 (bp, 2H, CH_2), 1.48 (s, 3H, CH_3), 1.52-1.54 (m, 2H, CH_2), 1.53 (s, 3H, CH_3), 1.69-1.72 (m, 2H, CH_2), 2.60 (s, 3H, CH_3), 2.80 (s, 3H, CH_3), 3.80 (t, 2H, CH_2, J = 6.0 Hz), 4.01 (t, 2H, CH_2, J = 6.0 Hz), 6.16 (s, 1H, ArH), 7.02 (d, 2H, ArH, J = 8.0 Hz), 7.13 (d, 2H, ArH, J = 8.0 Hz), 7.72-7.88 (m, 15 H, ArH, J = 8.0 Hz), 9.98 (s, 1H, CHO); ^{13}C NMR ($CDCl_3$, 100 MHz): δ 11.94, 13.27, 15.36, 22.84, 25.95, 27.73, 29.03, 29.84, 30.24, 68.13, 84.97, 115.60, 118.01, 118.86, 124.14, 126.27, 130.41, 130.65, 133.76, 142.94, 147.78, 156.09, 160.23, 161.65, 186.14 ppm.

Synthesis of compound 2. Compound **3** (0.72 g, 1 mmol), 2-cyanoactylanaline (0.32 g, 2 mmol) and piperazine (0.17 g, 2 mmol) were mixed in 20 mL DMF/methanol solvent (1/1 *v*/*v*). The obtained mixture was stirred at room temperature overnight. Then, the reaction mixture was poured into dry diethyl ether (200 mL) to form precipitates which were further purified on silica gel column chromatography (DCM-methanol) to obtain final product **2**. ^{1}H NMR ($CDCl_3$, 500 MHz): δ 9.98 (s, 1H), 8.00 (s, 1H), 7.84 – 7.76 (m, 15H), 7.70 – 7.66 (m, 10H), 7.12 (d, J = 8.43 Hz, 2H), 7.00 (d, J = 8.55 Hz, 2H), 6.13 (s, 1H), 4.09 (t, J = 6.59 Hz, 2H), 3.97 (t, J = 6.26 Hz, 2H), 2.79 (s, 2H), 2.59 (s, 2H), 2.25 – 2.21 (m, 2H), 2.02 – 1.96 (m, 2H), 1.79 – 1.46 (m, 20H) ppm.

Synthesis of probe 1. Compound **3** (0.72 g, 1 mmol), **8** (0.48, 1.5 mmol) and piperazine (0.17 g, 2 mmol) were mixed in 20 mL DMF/methanol solvent (1/1, *v*/*v*). The obtained mixture was stirred at room temperature for overnight. Then the reaction mixture was poured into dry diethyl ether (200 mL), to form precipitates which were further purified on silica gel column chromatography (DCM-methanol) to obtain final product **1** (0.5 g, 50%). ^{1}H NMR ($CDCl_3$, 400 MHz): δ 1.44 (s, CH_3, 3H), 1.47 (s, 3H, CH_3), 1.50 (t, 4H, CH_2, J = 4.0 Hz), 1.73 (t, 4H, CH_2, J = 4.0 Hz), 2.56 (s, 3H, CH_3), 2.63 (s, 3H, CH_3), 3.12-3.15 (m, 2H, CH_2), 3.31-3.34 (m, 2H, CH_2), 3.73-3.75 (m, 2H, CH_2), 3.96 (bp, 2H, CH_2), 6.09 (s, 1H, ArH), 6.96 (d, 2H, ArH, J = 8.0 Hz), 7.10 (d, 2H, ArH, J = 8.0 Hz), 7.55 (d, 2H, ArH, J = 8.0 Hz), 7.67 (m, 8H, ArH), 7.73 (m, 9H, ArH), 7.80 (s, 1H, CH), 7.83 (s, 1H, NH) ppm; ^{13}C NMR ($CDCl_3$, 100 MHz): δ 14.87, 15.40, 22.50, 22.88, 25.89, 29.07, 36.71, 42.02, 53.42, 68.12, 115.67, 118.00, 118.92, 120.49, 123.98, 129.21, 130.77, 135.90, 138.57, 140.53, 147.51, 153.43, 160.18, 162.76 ppm; Calculated $[M]^+$, $C_{55}H_{54}AsBF_2N_4O_2PS_2^+$, molecular weight: m/z Fw = 1021.27; Mass spectra ESI^+, found peak, 1021.50.

UV/Vis absorption and fluorescence spectroscopy. Stock solutions of **1** (1 mM) was prepared in DMSO solvent. UV/Vis absorption spectra of **1** were measured using a Perkin 3000 spectrophotometer (PE, USA), and fluorescent emission were recorded on a Horiba spectrofluorometer (Horiba) equipped with a xenon lamp, and regular PMT and an In/Ga/As detector for near infrared (window II) measurement.

Formation of reduced BSA (rBSA) and oxidized BSA (oBSA). rBSA was obtained by treating solution of BSA with 1.0 mM DTT overnight at 4 °C and oBSA was obtained by treating BSA with 100 μM H_2O_2 for 10 min at 25 °C. These samples were diluted 50 times with distilled water and then the proteins were recovered by precipitation in 50% acetone for 2 h at -20 °C.

Formation of oligomeric $A\beta_{1-42}$. Peptide (Beckham) with a concentration of 1 mg/mL was obtained by dissolving in 100% HFIP (1, 1, 1, 3, 3, 3-hexafluoro-2-propanol) and incubated at room temperature for 3 days with vortex at moderate speed. This was sonicated for 10 min while the tube is held in the upright position. And then sample was dried under a gentle nitrogen gas stream and vial was capped immediately. Aβ peptide stock sol. (50 μg) was suspended in 13 μL DMSO and 50 μL of DMEM was added, mixed and incubated for 2 h (5% CO_2, 37 °C). This sample has 63 μL total volume and 100 μM β-amyloid in oligomeric form.

Cell culture. HeLa cells were cultured at moderate density in DMEM medium. All culturing media were supplemented with penicillin (100 units/mL), 10% (*v*/*v*) FBS (WelGene) and streptomycin (100 mg/mL) under 5% CO_2 atmosphere and 95% humidity at 37 °C.

Confocal microscopy. 24 hours before imaging on a microscope, the cells were seeded on cover glass bottom dish (SPL Lifesciences Co., Ltd.) which was incubated in a humidified atmosphere containing 5% (*v*/*v*) CO_2 at 37 ^{o}C. Cell images were obtained using confocal laser scanning microscopy (Leica SP8, Leica, Germany). Other information is available in the figure captions.

SDS-PAGE and fluorescence image of gels. The selectivity of compound **1** towards proteins or cells was verified by 10% SDS-PAGE. Samples were treated with **1** in de-ionized water (DW) or DMEM at 5% CO_2 and 95% humidity at 37 ^{o}C for 1 hour. After labeling, the samples were precipitated with 50% (*v*/*v*) acetone for 2 hours at -20 ^{o}C and then mixed with SDS-PAGE loading buffer with tris (2-carboxyethyl) phosphine (TCEP) and the electrophoresis was started immediately. The gel was imaged by a fluorescent scanner (Typhoon FLA 9400, GE) upon 488 nm excitation with a band path filter

ranging from 500 nm to 540 nm. The same gel was stained *via* Coomassie brilliant blue (CBB) G250 after the fluorescent image was obtained.

Mass spectrometry. The trypsin digests (5.0 μL) were prepared in buffer A (H_2O/acetonitrile/HCO_2H; 95:5:0.2, *v*/*v*/*v*) and then injected into an analytical column (3.0 μm particle size, Atlantis™ dC18, Waters) equipped with C_{18} reversed-phase of 75 μm i.d. × 150 mm with an integrated electrospray ionization Silica Tip™. The peptides were desalted in a line before separation through a trap column (0.35 × 50 mm, OPTI-PAK™ C_{18}, Waters) and rinsed by a linear gradient of buffer Bof 5-80% (ACN/water/formic acid; 95 : 5 : 0.2, *v*/*v*/*v*) for 2 hours. A split/splitless inlet speed of 200 nL. $Min^{-1}$was set and the capillary voltage (3 kV) was employed to the HPLC mobile phase prior to spraying. The mass spectrometer was set up to measure scan cycles consisting of one MS scan followed by MS/MS scans of the most abundant ions in each scan in 10 seconds. The obtained spectra were automatically analyzed through Proteo Lynx Global Server 3.0.2 (Waters, Manchester, UK) and then matched against amino acid sequences in human Swiss Prot database (version 57.8). The search parameters were shown as follows: Dalton tolerance (0.2) for peptide and fragments; digested with trypsin enzyme was up to one missed cleavage allowed, de-amidation (NQ), propionamidation, oxidation (M) or cabamidomethylation (C) were set as a variable modification. Results were recorded using probability-based Mowse score (Protein score is -10 × log (*p*), where *p* is the probability that the obtained match is a random event. Protein with scores greater than 20 is counted to be significant ($p < 0.05$)).

Western blotting. The same volume of subcellular fraction was mixed with buffer solution of 5× Laemmle and then boiled for 5 min. The obtained mixtures were separated on 10% SDS (SDS-PAGE) and then transferred to nitrocellulose membranes which were incubated with a blocking buffer composed of 5% nonfat milk or 1% BSA in Tris-buffered saline with 0.5% Tween-20) for 1 hour with

shaking at room temperature. The blots were cultured with the primary antibodies in the blocking buffer solution at 4 °C for overnight. The specific immune reactive proteins were observed by Tanon gel Imaging/Analysis System (Tanon-5220S, China).

STED super resolution imaging. All super-resolution experiments were achieved on a custom-built STED microscope system. For excitation section, a super-continuum laser power with pulse rate of 80 MHz was applied. The excitation wavelength of 514 nm and its fluorescence intensity was adjusted by an acousto-optical tunable filter (AOTF). A continuous-wave of 592 nm (MPB Communications Inc., Montreal, Canada) as the depletion beam (STED beam) was used on this system. Both laser beams pass through an optical fiber with polarization-maintain and were focused into a scanner. The STED beam was induced through an easy STED phase plate (B-Halle, Berlin, Germany) on aback focal plane of STED objective (HCX PL APO CS_2 100×/1.40 oil, Leica Microsystems). The fluorescence of back-propagating sample was collected by the same objective and passed through the detection path by a direction beam splitter, and then refined by a pinhole with diameter of 151.6 μm (~ 1 Airy unit). The fluorescence emission ranging from 520 to 560 nm was collected on the hybrid detector. Images were obtained *via* time-gated detection of the gate opening upon excitation and the STED laser passing through. Acquisition of images was generally accomplished with multiple lines and frame accumulations. Here a typical acquisition set was carried out accumulate four lines and two frames totally with a pixel dwell time (2.4 μs), the field view of images was set at 26.53 μm × 26.53 μm with 1024 × 1024 pixels and each pixel size was 6 nm.

Acknowledgments

This research was supported by the National Natural Science Foundation of China (No. 21406125),the National Basic Research Program of China (No. 2015CB352005); Guangdong Natural Science

Foundation Innovation Team (No. 2014A030312008); Hong Kong, Macao and Taiwan cooperation innovation platform & major projects of international cooperation in Colleges and Universities in Guangdong Province (No. 2015KGJHZ002); and the Ministry of Science, ICT & Future Planning (MSIP) of National Research Foundation of Korea (No. 2009-0081566, JSK), (No. 2015R1A5A1037656, C.K.) and (No. 2014R1A6A3A04058006, DHK).

Associated Content

Supporting information

The Supporting Information is available free of charge on the ACS Publications website at DOI: 10.1021/acs.bioconjchem.xx

Materials for the synthesis, Supporting absorbance and emission spectra, Supporting confocal and super-resolution cell images, Western blot analysis of organelle fractions and NMR spectra (PDF)

References

1. Ko, M., An, J., Bandukwala, H. S., Chavez, L., Aijo, T., Pastor, W. A., Segal, M. F., Li, H., Koh, K. P., Lahdesmaki, H., et al. (**2013**) Modulation of TET2 expression and 5-methylcytosine oxidation by the CXXC domain protein IDAX, *Nature 497*, 122-126.
2. Lu, J., and Holmgren, A. (**2014**) The thioredoxin superfamily in oxidative protein folding, *Antioxid. Redox. Signal 21*, 457-470.
3. Putker, M., Vos, H. R., and Dansen, T. B. (**2014**) Intermolecular disulfide-dependent redox signalling, *Biochem. Soc. Trans. 42*, 971-978.

4. Messens, J., and Collet, J. F. (**2013**) Thiol-Disulfide Exchange in Signaling: Disulfide Bonds As a Switch, *Antioxid*. *Redox*. *Signal 18*, 1594-1596.

5. Requejo, R., Chouchani, E. T., James, A. M., Prime, T. A., Lilley, K. S., Fearnley, I. M., and Murphy, M. P. (**2010**) Quantification and identification of mitochondrial proteins containing vicinal dithiols, *Arch*. *Biochem*. *Biophys*. *504*, 228-235.

6. Zhang, X. W., Yan, X. J., Zhou, Z. R., Yang, F. F., Wu, Z. Y., Sun, H. B., Liang, W. X., Song, A. X., Lallemand-Breitenbach, V., Jeanne, M., et al. (**2010**) Arsenic Trioxide Controls the Fate of the PML-RAR alpha Oncoprotein by Directly Binding PML, *Science 328*, 240-243.

7. Zschauer, T. C., Matsushima, S., Altschmied, J., Shao, D., Sadoshima, J., and Haendeler, J. (**2013**) Interacting with thioredoxin-1--disease or no disease? *Antioxid*. *Redox. Signal 18*, 1053-1062.

8. Sugatani, J., Steinhelper, M. E., Saito, K., Olson, M. S., and Hanahan, D. J. (**1987**) Potential involvement of vicinal sulfhydryls in stimulus-induced rabbit platelet activation, *J*. *Biol*. *Chem*. *262*, 16995-17001.

9. Voehler, M. W., Eoff, R. L., McDonald, W. H., Guengerich, F. P., and Stone, M. P. (**2009**) Modulation of the structure, catalytic activity, and fidelity of African swine fever virus DNA polymerase X by a reversible disulfide switch, *J*. *Biol*. *Chem*. *284*, 18434-18444.

10. Cohen, T. J., Hwang, A. W., Unger, T., Trojanowski, J. Q., and Lee, V. M. (**2012**) Redox signalling directly regulates TDP-43 via cysteine oxidation and disulphide cross-linking, *EMBO J. 31*, 1241-1252.

11. Requejo, R., Chouchani, E. T., James, A. M., Prime, T. A., Lilley, K. S., Fearnley, I. M., and Murphy, M. P. (**2010**) Quantification and identification of mitochondrial proteins containing vicinal dithiols, *Arch*. *Biochem*. *Biophys*. *504*, 228-235.

12. Neumann, D., Buckers, J., Kastrup, L., Hell, S. W., and Jakobs, S. (**2010**) Two-color STED microscopy reveals different degrees of colocalization between hexokinase-I and the three human VDAC isoforms, *PMC Biophys*. *3*, 4.

13. Colombini, M. **(2004**) VDAC: The channel at the interface between mitochondria and the cytosol, *Mol*. *Cell*. *Biochem*. *256*, 107-115.

14. Shen, S., Li, X. F., Cullen, W. R., Weinfeld, M., and Le, X. C. (**2013**) Arsenic binding to proteins, *Chem*. *Rev*. *113*, 7769-7792.

15. Zhang, X., Yang, F., Shim, J. Y., Kirk, K. L., Anderson, D. E., and Chen, X. (**2007**) Identification of arsenic-binding proteins in human breast cancer cells, *Cancer Lett*. *255*, 95-106.

16. Huang, C., Yin, Q., Zhu, W., Yang, Y., Wang, X., Qian, X., and Xu, Y. (**2011**) Highly selective fluorescent probe for vicinal-dithiol-containing proteins and in situ imaging in living cells, *Angew*. *Chem*. *Int*. *Ed*. *50*, 7551-7556.

17. Wang, Y., Zhong,Y., Wang, Q., Yang, X.-F., Li, Z., and Li, H. **(2016)** Ratiometric Fluorescent Probe for Vicinal Dithiol-Containing Proteins in Living Cells Designed via Modulating the Intramolecular Charge Transfer–Twisted Intramolecular Charge Transfer Conversion Process, *Anal. Chem. 88*, 10237–10244.

18. Liu, F., Liu, H.-J., Liu, X.-J., Chen, W., Wang, F., Yu, R.-Q. and Jiang, J.-H. **(2017)** Mitochondrion-targeting, environment-sensitive red fluorescent probe for highly sensitive detection and imaging of vicinal dithiol-containing proteins, *Anal. Chem. 2017*, 89, 11203–11207.

19. Huang, C., Jia, T., Tang, M., Yin, Q., Zhu, W., Zhang, C., Yang, Y., Jia, N., Xu, Y., and Qian, X. (**2014**) Selective and ratiometric fluorescent trapping and quantification of protein vicinal dithiols and in situ dynamic tracing in living cells, *J*. *Am*. *Chem*. *Soc*. *136*, 14237-14244.

20. Banci, L., Bertini, I., Calderone, V., Cefaro, C., Ciofi-Baffoni, S., Gallo, A., and Tokatlidis, K. (**2012**) An Electron-Transfer Path through an Extended Disulfide Relay System: The Case of the Redox Protein ALR, *J. Am. Chem. Soc. 134*, 1442-1445.

21. Herrmann, J. M., and Riemer, J. (**2012**) Mitochondrial Disulfide Relay: Redox-regulated Protein Import into the Intermembrane Space, *J. Biol. Chem. 287*, 4426-4433.

22. Yang, Z., He, Y., Lee, J. H., Park, N., Suh, M., Chae, W. S., Cao, J. F., Peng, X. J., Jung, H., Kang, C., and Kim, J. S. (**2013**) A Self-Calibrating Bipartite Viscosity Sensor for Mitochondria, *J. Am. Chem. Soc. 135*, 9181-9185.

23. Hoye, A. T., Davoren, J. E., Wipf, P., Fink, M. P., and Kagan, V. E. (**2008**) Targeting mitochondria, *Acc. Chem. Res. 41*, 87-97.

24. Kuo, C. Y., Wang, H. C., Kung, P. H., Lu, C. Y., Liao, C. Y., Wu, M. T., and Wu, C. C. (**2014**) Identification of CalDAG-GEFI as an intracellular target for the vicinal dithiol binding agent phenylarsine oxide in human platelets, *Thromb. Haemost. 111*, 892-901.

25. Zhu, H., Fan, J., Du, J. and Peng, X. **(2016)** Fluorescent Probes for Sensing and Imaging within Specific Cellular Organelles, *Acc. Chem. Res. 49*, 2115-2126.

26. Xu, W., Zeng, Z., Jiang, J.-H., Chang Y.-T. and Yuan, L. **(2016)** Discerning the Chemistry in Individual Organelles with Small-Molecule Fluorescent Probes, *Angew. Chem. Int. Ed. 55*, 13658-13699.

27. Ning, P., Wang, W., Chen, M., Feng, Y., Meng, X. **(2017)** Recent advances in mitochondria- and lysosomes-targeted small-molecule two-photon fluorescent probes, *Chin. Chem. Lett. 28*, 1943-1951

28. Sheehan, J. P., Swerdlow, R. H., Miller, S. W., Davis, R. E., Parks, J. K., Parker, W. D., and Tuttle, J. B. (**1997**) Calcium homeostasis and reactive oxygen species production in cells transformed by mitochondria from individuals with sporadic Alzheimer's disease, *J. Neurosci. 17*, 4612-4622.

29. Lustbader, J. W., Cirilli, M., Lin, C., Xu, H. W., Takuma, K., Wang, N., Caspersen, C., Chen, X., Pollak, S., Chaney, M., et al. (**2004**) ABAD directly links Aβ to mitochondrial toxicity in Alzheimer's disease, *Science 304*, 448-452.

30. Mari, M., Morales, A., Colell, A., Garcia-Ruiz, C., Kaplowitz, N., and Fernandez-Checa, J. C. (**2013**) Mitochondrial glutathione: features, regulation and role in disease, *Biochim*. *Biophys*. *Acta 1830*, 3317-3328.

31. De Pinto, V., Reina, S., Gupta, A., Messina, A., and Mahalakshmi, R. (**2016**) Role of cysteines in mammalian VDAC isoforms' function, *Biochim*. *Biophys*. *Acta 1857*, 1219-1227.

32. Reina, S., Checchetto, V., Saletti, R., Gupta, A., Chaturvedi, D., Guardiani, C., Guarino, F., Scorciapino, M. A., Magri, A., Foti, S., et al. (**2016**) VDAC3 as a sensor of oxidative state of the intermembrane space of mitochondria: the putative role of cysteine residue modifications, *Oncotarget*. *7*, 2249-2268.

33. Yao, C. X., Behring, J. B., Shao, D., Sverdlov, A. L., Whelan, S. A., Elezaby, A., Yin, X. Y., Siwik, D. A., Seta, F., Costello, C. E., et al. (**2015**) Overexpression of catalase diminishes oxidative cysteine modifications of cardiac proteins, *Plos One 10*, e0144025.

34. Maurya, S. R., and Mahalakshmi, R. (**2014**) Cysteine residues impact the stability and micelle interaction dynamics of the human mitochondrial β-barrel anion channel hVDAC-2, *Plos One 9*, e92183.

35. Baines, C. P., Kaiser, R. A., Sheiko, T., Craigen, W. J., and Molkentin, J. D. (**2007**) Voltage-dependent anion channels are dispensable for mitochondrial-dependent cell death, *Nat*. *Cell*. *Biol*. *9*, 550-555.

36. Cheng, E. H., Sheiko, T. V., Fisher, J. K., Craigen, W. J., and Korsmeyer, S. J. (**2003**) VDAC2 inhibits BAK activation and mitochondrial apoptosis, *Science 301*, 513-517.

37. Wimmer, N., Robinson, J. A., Gopisetty-Venkata, N., Roberts-Thomson, S. J., Monteith, G. R., and Toth, I. (**2006**) Anti-proliferative effects of novel glyco-lipid-arsenicals (III) on MCF-7 human breast cancer cells, *Med. Chem. 2*, 79-87.

Table of Content

Realizing the significant roles of vicinal-dithiol proteins (VDPs) in maintaining the cellular redox homeostasis and their implication in many diseases, a smart arsenate based fluorescent probe **1** was designed which can preferentially target the mitochondrial membrane-bound VDPs, especially Voltage-dependent anion channel (VDAC2) as demonstrated by ‘‘in vitro’’ studies such as co-localization, stimulated emission depletion (STED) super-resolution imaging, proteomic MS/MS analysis and by western blot analysis. As far we know, our probe represents a rare example of fluorescence labelling the mitochondrial membrane-bound VDPs. We believe that these findings can provide a new way to construct VDPs-specific fluorescent probes in order to gain deeper understanding of their roles in mitochondrial-related disorders.

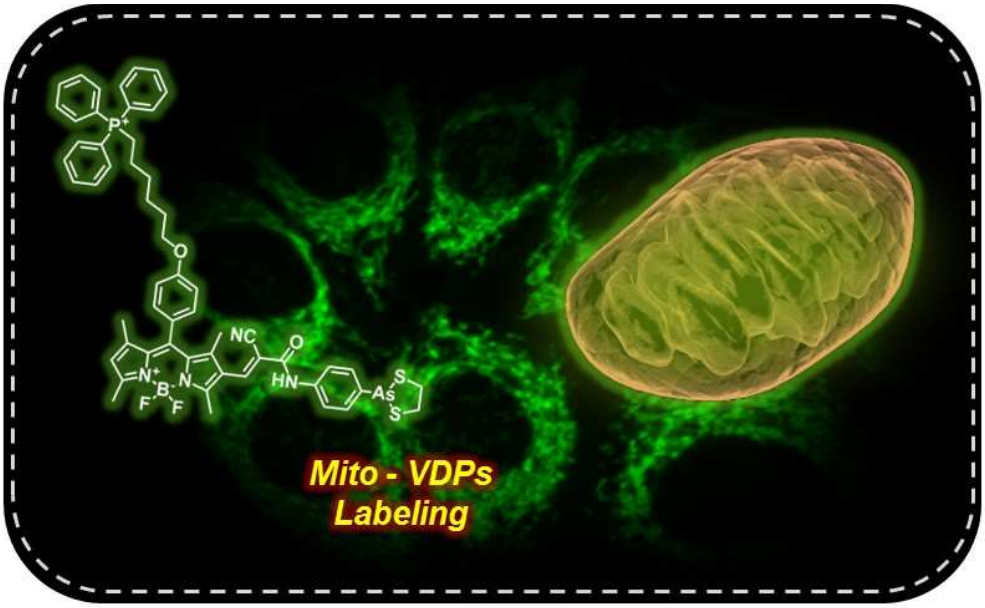
Mito - VDPs
Labeling